Preparation and characterisation of ceramic-faced metal–ceramic interpenetrating composites for impact applications

Hong Chang · Jon Binner · Rebecca Higginson ·
Paul Myers · Peter Webb · Gus King

Abstract This article accesses the impact performance of ceramic-faced, metal–ceramic interpenetrating composites (IPCs) produced in situ from infiltrating ceramic foams with a molten aluminium–magnesium alloy. The approach had two variations, viz., the production of a metal bond between a ceramic front face and backing IPC and the creation of a ceramic bond. The impact performance of metal-bonded IPCs was evaluated using both split Hopkinson's pressure bar (SHPB) and depth of penetration (DoP) techniques. With a 4-mm thick Al_2O_3 front face and an 8-mm thick IPC backing, the DoP was zero. In one case, a sample survived fundamentally intact with only spall damage to the dense Al_2O_3 front face. The resulting damage was thoroughly assessed using a range of techniques, including polarized light microscopy, scanning electron microscopy (SEM), 3D MicroCT and transmission electron microscopy (TEM). The metal phase deformed as a result of the formation of large numbers of dislocations, whilst the ceramic phase accommodated the deformation via localised cracking. Metal bridges across the cracks formed, increasing the damage tolerance of the IPCs. The metal bond between the ceramic front face and the IPC was also observed to withstand the impact of the armour piercing rounds without any sign of debonding occurring.

H. Chang · J. Binner · R. Higginson
Department of Materials, Loughborough University,
Leicestershire LE11 3TU, UK

P. Myers
Dyson Thermal Technologies, Sheffield S17 3BL, UK

P. Webb · G. King
Permali (Gloucester) Ltd, Gloucester GL1 5TT, UK

H. Chang (✉)
College of Engineering, Mathematics and Physical Sciences,
University of Exeter, Exeter EX4 4QF, UK
e-mail: Maggie.chang10@yahoo.co.uk

Introduction

Light weight armour materials are becoming increasingly important due to the need for increased personnel protection and also the move towards lighter, faster, more fuel efficient vehicles. For an armour tile to be effective it needs both high penetration resistance and the capability of withstanding more than a single impact, i.e. multi-hit potential. Whilst ceramics such as Al_2O_3, SiC and TiB_2 are attractive materials for ballistic applications in terms of their abrasion resistance (which can blunt the incoming projectiles and absorb the energy, hence defeating the threat) they have poor multi-hit potential, shattering after as little as one impact and need to be replaced [1]. Whilst such deficiencies can be at least partially addressed by using a mosaic approach and constraint, ceramic armour is generically fairly heavy.

Most armour systems are made up of composite layers of a number of materials to obtain the maximum protection for the minimum mass [2]. However, when there is a ceramic front face, acoustic impedance mismatches at the resulting interface can be a cause of significant problems since the stress waves from the ballistic event are reflected back inside the ceramic as tensile waves, causing its rapid destruction [3, 4].

Metal matrix composites (MMCs) have been shown to display improved strength, stiffness, hardness, wear and abrasion resistance, lower thermal expansion coefficients and better resistance to elevated temperatures and creep compared to the matrix metal, whilst retaining adequate electrical and thermal conductivity, ductility, impact and

oxidation resistance [1, 5, 6]. They are starting to be used in a variety of applications, including the aerospace and defence industries [7–11]. 3–3 interpenetrating composites (IPCs), consisting of two three-dimensionally interpenetrating matrices of different phases, are interesting materials with potentially superior properties compared with traditional dispersed phase composites [12]. One of the most widely used methods to fabricate metal–ceramic IPCs is via the infiltration of molten metals into ceramic foams or powder beds [13]. Whilst infiltration under pressure, such as squeeze casting, offers high efficiency, it is difficult to fabricate complex-shaped components and the pressures involved risk damaging the ceramic preform. Pressureless infiltration approaches avoid these limitations [14, 15]. By careful control of the thermo-atmospheric cycle and the use of precursor coatings, a range of molten aluminium alloys can be successfully infiltrated into a number of ceramic foam compositions, including alumina, mullite, silicon carbide and silicon nitride [16–19].

Previous work [20] has demonstrated that whilst metal–ceramic IPCs are not suitable for resisting high velocity, armour piercing (AP) rounds on their own, when bonded to a 3 mm thick, dense Al_2O_3 front face, significant deflection was observed and the depth of penetration (DoP) was reduced. The objective of the present work was to develop a route to the in situ manufacture of IPCs bonded to a dense ceramic front face, using the pressureless infiltration technique, with the aim of reducing the acoustic impedance mismatch between the ceramic and the aluminium backing. The ballistic properties were evaluated using both split Hopkinson's pressure bar (SHPB) and DoP techniques. The damage to the samples after testing was thoroughly assessed using both optical and electron microscopy.

Experimental

Processing

The metal infiltrant, an Al–8Mg alloy, was prepared from commercially pure Al and an Mg–Al master alloy, AZ81, using an approach described in detail elsewhere [21]. For both 'metal-bonded' and 'ceramic-bonded' composite systems, the IPCs were made from alumina foams measuring ⌀ 50 × 8 mm in size with a density of either 25 or 45% of theoretical and average cell diameters of 50–150 μm. They were manufactured by Dyson Thermal Technology, Sheffield, UK, using a gel-casting technique [22]. ⌀ 50 × 4 mm thick, dense, slip cast alumina discs were also made from submicron Al_2O_3 powder (CT3000, SG, Alcoa Industrial Chemicals Europe, Frankfurt, Germany) and sintered to >99% of theoretical density. To produce the 'ceramic-bonded' ceramic-IPC samples, Dyson Thermal Technology sintered the 4-mm thick green slip cast alumina discs to one face of the 45% ceramic foams. Note that differential shrinkage between the foam and the slip cast discs prevented bonding for foams with a density lower than 45% of theoretical.

For the 'ceramic-bonded' ceramic-IPC samples, the dense ceramic/ceramic foam couples were placed in an alumina boat with the dense ceramic layer at the bottom and a disc of the Al–8Mg alloy on top of the foam, Fig. 1a. During the subsequent heat treatment described below, the metal melted and infiltrated the foam forming the IPC in situ. For the 'metal-bonded' ceramic-IPC samples the arrangement of the materials was the same, Fig. 1a, though the 25% dense foams were used and the dense ceramic was not presintered to the foam. Now, when the metal melted and infiltrated the foam forming the IPC it also formed a thin metal layer between the IPC, Fig. 1b, and effectively bonded the front face to the IPC in a single process step.

The infiltration process took place in pure N_2 (oxygen free, BOC Gases, Manchester, UK) at 915 °C with a holding time of 30–60 min being used to obtain complete infiltration with the alloy penetrating through the foam as a result of capillary action [21]. Heating to and cooling from 915 °C was performed in an argon atmosphere using a heating rate of 20 °C min^{-1} and a cooling rate of 10 °C min^{-1}. The atmosphere was changed to nitrogen once the temperature stabilised at 915 °C and then back to argon once infiltration was complete. The latter could be ascertained by visual examination of the process through a gas-tight window at one end of the tube furnace.

Impact testing

Initial evaluation of the high strain rate characteristics of the composites was carried out using the SHPB technique on samples measuring 9 mm in diameter and 4.5 mm in thickness. The impact from a striker bar, transmitted to the

Fig. 1 a The arrangement for producing in situ IPCs bonded attached to a dense ceramic layer and b the resulting composite system with a thin layer of metal bonding the ceramic to the IPC (not to scale)

samples via an incident bar, generated an incident wave, part of which was reflected back whilst the rest was transmitted through the composite. The stress–strain curve of the composite was obtained from the analysis of the incident wave, the reflective wave and the transmitted wave [23]. The DoP ballistic evaluation of the composites was performed by Permali (Gloucester) Ltd. using 7.62 mm, steel, AP rounds at a velocity of 700 ± 20 m s^{-1}. The composites were glued onto an aluminium backing with a thickness of ~ 50 mm; the residual energy of the bullet after passing through the target composite was indicated quantitatively by the DoP of the round into the backing. This was ascertained by cutting the backing aluminium in half to reveal the DoP. For both techniques, the dense ceramic front faces of the samples were positioned facing the impact.

Microstructure characterisation and damage assessment

For scanning electron microscopy (SEM) observation (LEO 1530VP, Carl Zeiss SMT, Oberkochen, Germany), fragments from the tested samples from both techniques were ground and polished metallographically using diamond paste and then given a final polish using 0.02 µm colloidal silica. For polarized light microscopy, the samples were anodized using 5% fluroboric acid at 20 V. TEM samples from the metal–ceramic interface were specifically prepared from both SHPB and DoP tested samples using a Dual Beam Focused Ion Beam (Nova 600 Nanolab, FEI Company, Hillsboro, OR, USA); in the latter, the samples were prepared from near the impact site. The thin films were then examined in a JEOL 2000FX. The physical structure of the samples as well as the damage after the ballistic testing were also observed using a micro-focus X-ray and Computer Tomography (micro CT) inspection system (XT H 225, Metris, Belgium).

Results and discussion

Processing

A typical cross-sectional micrograph of the interface between the dense ceramic front face and the IPC for a 'metal-bonded' ceramic-IPC is shown in Fig. 2a. It reveals that the process worked extremely well with the dense ceramic face being bonded onto the IPC with no gaps or residual porosity. The thickness of the metal bonding layer was in the range 100–300 µm along the length of the interface. A typical SEM micrograph of the IPC itself, which also appears at the bottom of Fig. 2a, is shown in Fig. 2b; it can be seen that the foam was essentially fully infiltrated in the same processing step. A few residual pores may be observed at localised positions, these were either a

result of metal shrinkage or a result of the very small number of closed pores in the foam struts.

A microCT image of a 'ceramic-bonded' ceramic-IPC is shown in Fig. 3a; it can be seen that the ceramic and the foam were seamlessly bonded, though there is also evidence for some residual porosity in the 'dense' ceramic layer. However, after infiltration, Fig. 3b, it can be seen that whilst the molten metal infiltrated evenly from the periphery of the ceramic foam, the centre of the foam was not infiltrated. This might have been due to gas becoming trapped between the molten alloy front and the ceramic face; drilling fine holes in the front face would probably have solved this problem. It is also probable that the use of a foam as dense as 45% of theoretical will not have aided the infiltration process. Either way, the lack of full infiltration of these foams meant that they were not used for further testing; the degree of success achieved with the 'metal-bonded' approach meant that further effort was not expended trying to improve the degree of infiltration for the 'ceramic-bonded' approach.

Ballistic evaluation

Representative SHPB results are shown in Fig. 4. In Fig. 4a, the Al–Mg alloy, included for comparison, showed a continuous increase in the stress with strain as expected as a result of strain/work hardening. Although the metal-bonded ceramic-IPCs contained both a ceramic skeleton in the IPC as well as the ceramic facing, they yielded at 4–6% strain then displayed plastic deformation, Fig. 4b, behaviour typical of a metallic material. As expected, the maximum stress of the ceramic-faced IPCs was significantly higher than that of the alloy on its own, viz., ~ 530 versus 370 MPa. Observation of the samples following the tests showed that the ceramic front face fractured during the test; this may correspond to the 'yield point' at ~ 400 MPa in Fig. 4b. The further increase in stress following this initial 'yield point' was probably a result of the plastic deformation of the IPC. Based on previous work on the SHPB testing of metal–ceramic IPCs [20], it suggests that the interpenetrating ceramic structure suffered the initiation of microcracking and fracture. Although the IPCs contained rigid ceramic struts, the samples plastically deformed with only localised fracture in the ceramic phases. It should be noted that Fig. 4 only presents the performance of the components at relatively low strain rates as attempts at using higher strain rates resulted in damage to the striker and transmitter bars—suggesting that the metal-bonded ceramic-IPCs may offer excellent ballistic properties.

Typical images of the metal-bonded ceramic-IPCs after the DoP tests are shown in Fig. 5. From Fig. 5a, the sample fractured into several pieces and detached completely from the backing, however, the ceramic front face remained
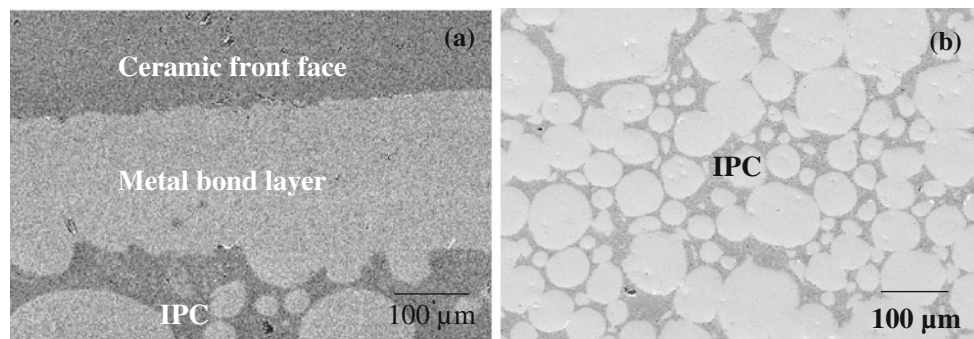
Fig. 2 SEM micrographs of **a** the interface between the IPC and the dense ceramic front face for the 'metal-bonded' ceramic-IPC; **b** the IPC itself

Fig. 3 Typical MicroCT images of a ceramic-bonded ceramic-IPC sample **a** prior to infiltration and **b** after infiltration
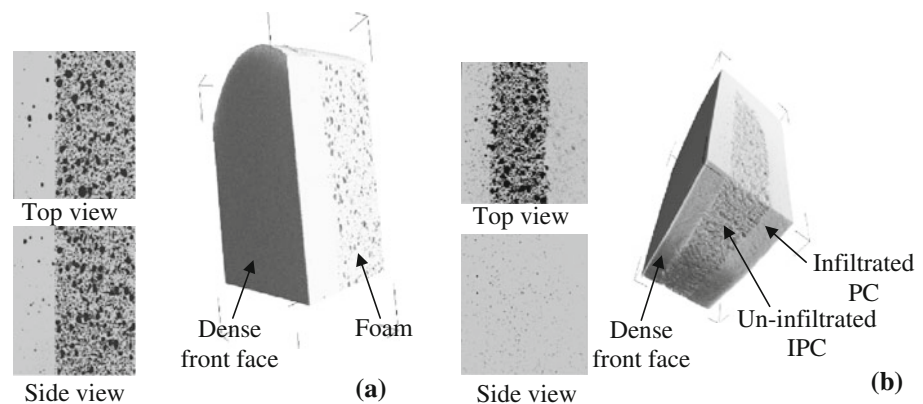

Fig. 4 Stress-strain curves (Red: engineering stress–strain; blue: true stress–strain) of **a** Al–Mg alloy; **b** metal-bonded ceramic-IPCs. Both at ~ 1200 s^{-1}
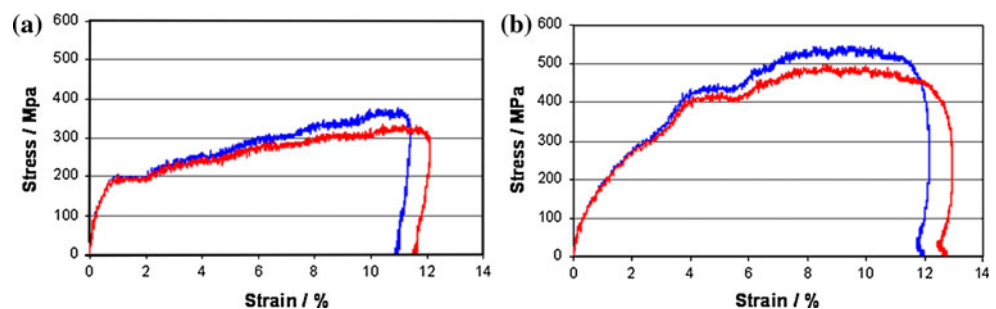
largely bonded to the IPC backing. In Fig. 5b, again, the sample fractured into several pieces, though some remained attached to the backing this time. Once again, the front face remained bonded to the IPC. To summarize, although the samples generally detached from the backing and fractured into several pieces, there was no penetration into the Al alloy backing, i.e. the DoP was zero for every sample. One sample (Fig. 5c), in particular, survived fundamentally intact with only the Al$_2$O$_3$ dense facing cracking perpendicular to the impact and the front spalling off. These results significantly exceed the tests performed earlier on the Al–Mg/15%Al$_2$O$_3$ IPCs ($\varnothing$ 50 × 8 mm) to which a $\varnothing$ 10 × 3 mm slip cast Al$_2$O$_3$ disk had been attached by the same method [14], though the larger size of

the Al$_2$O$_3$ disks in the current research could have improved the ballistic performance of the samples. Mass efficiency calculations of the metal-bonded IPCs yielded a value of 2.6, which is a favourable result [24].

The ballistic properties of ceramic-faced armours have been widely studied [25–28]. The presence of a functionally gradient layer between the ceramic front face and metal back face can make the acoustic impedance change less abrupt, resulting in less damage from reflected tensile forces [3]. It has also been reported that when a porous ceramic preform is infiltrated by aluminium, the presence of the aluminium skeleton can improve the residual strength after impact [29]. In the present work, it is believed that the attachment of the IPC to the dense Al$_2$O$_3$
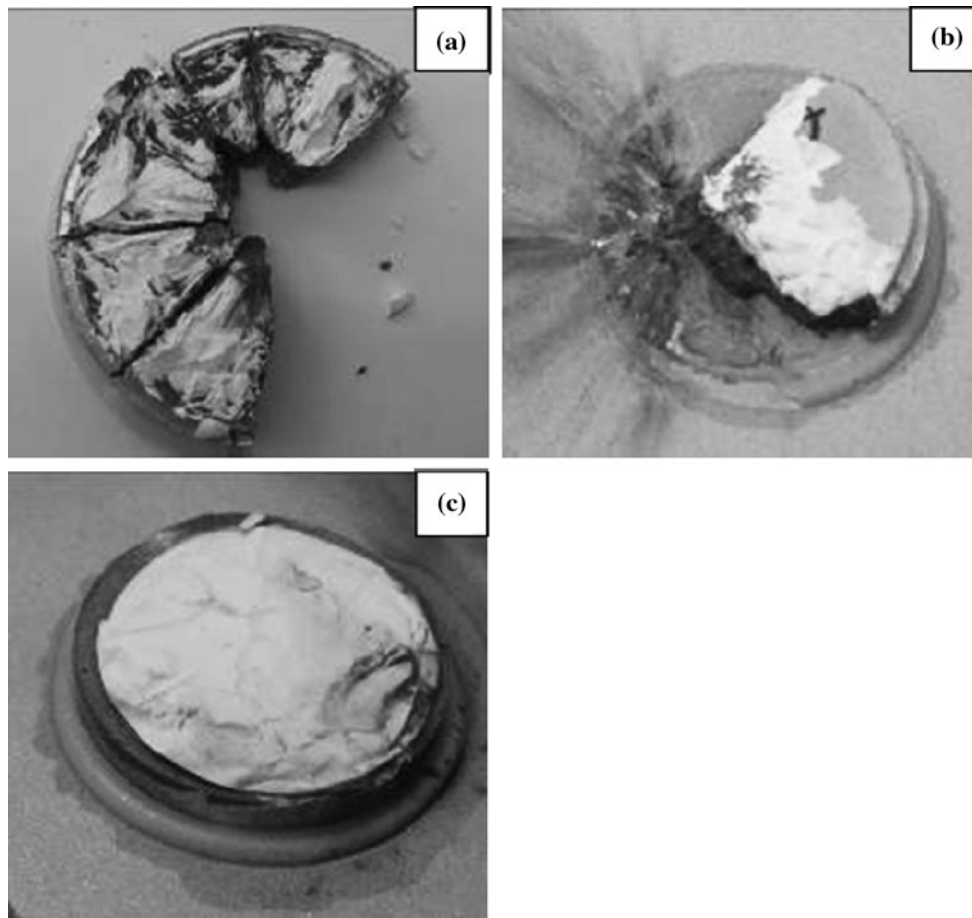
Fig. 5 Some typical metal-bonded ceramic-IPCs after ballistic testing using steel tipped, armour piercing rounds at 700 ± 20 m s^{-1}

layer may have reduced the acoustic impedance mismatch, resulting in the superior ballistic performance of the samples.

Microstructure characterisation and damage assessment

A typical optical image and SEM micrograph of an IPC after SHPB are shown in Fig. 6. The deformation of the original spherical cells into ellipses may be clearly seen,

localised fracture in the ceramic phase occurring to accommodate the deformation. No macroscopic metal–ceramic interfacial debonding was observed, a result that was expected. As a result of the protection offered by the ceramic front facing, less deformation and cracking was observed in the IPCs that were bonded to the dense ceramic layers.

A 3D MicroCT image of a metal-bonded ceramic-IPC after DoP testing (the sample in Fig. 5c) is shown in Fig. 7.
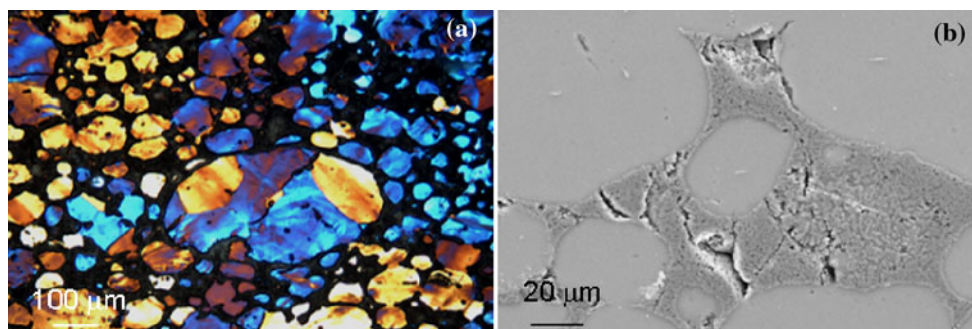

Fig. 6 a Optical and **b** SEM micrographs of an IPC after SHPB testing at 1200 s^{-1}

Fig. 7 MicroCT image of the metal-bonded ceramic-IPC shown in Fig. 5c

Topview

Side view

IPC

Dense front face
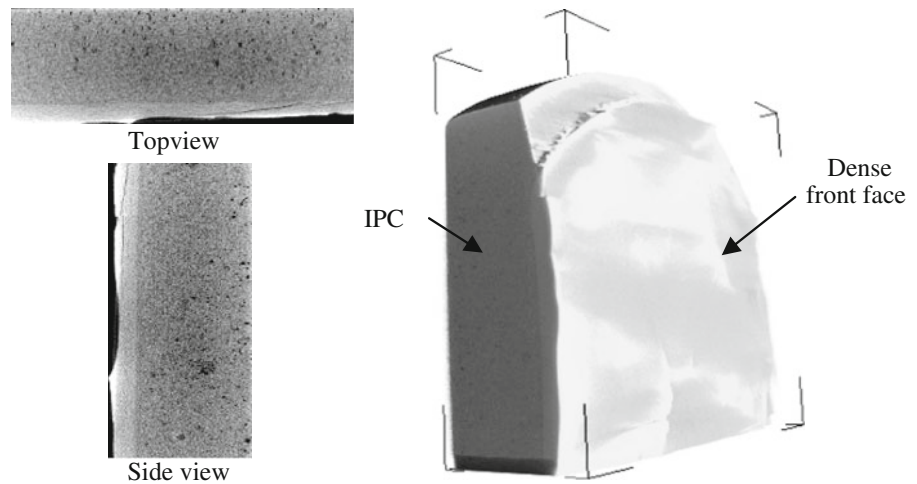
It clearly shows that no damage was caused to the IPC layer beneath the ceramic front face and that the latter was still firmly bonded to the IPC beneath it despite being hit by a steel tipped, 7.62 mm, AP round at 700 m s⁻¹.

Typical cross-sectional SEM micrographs of a fragment from Fig. 5a are shown in Fig. 8a and b. These show no evidence of interfacial debonding, though the ceramic front face is cracked, presumably as a result of reflections of
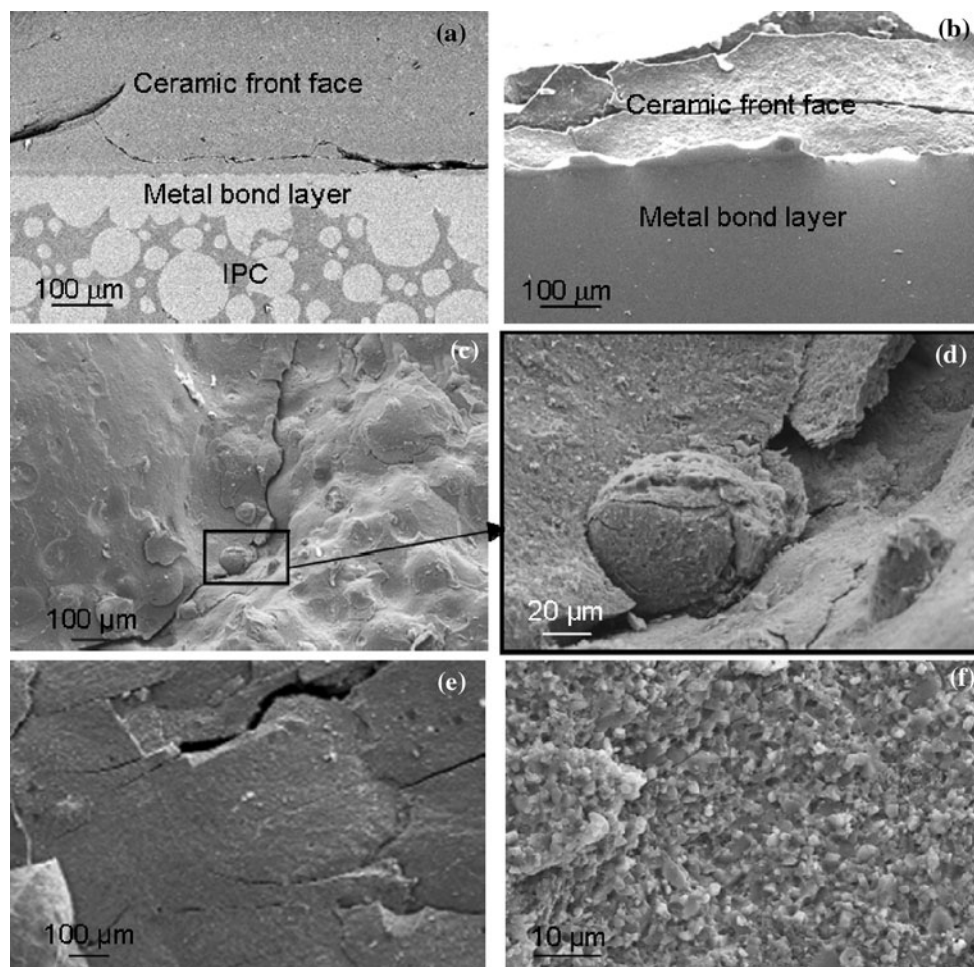
Fig. 8 SEM micrographs of the metal-bonded ceramic-IPC after DoP: **a**, **b** cross-section; **c**, **d** fracture surface along a radial crack; **e**, **f** top surface of the ceramic front face
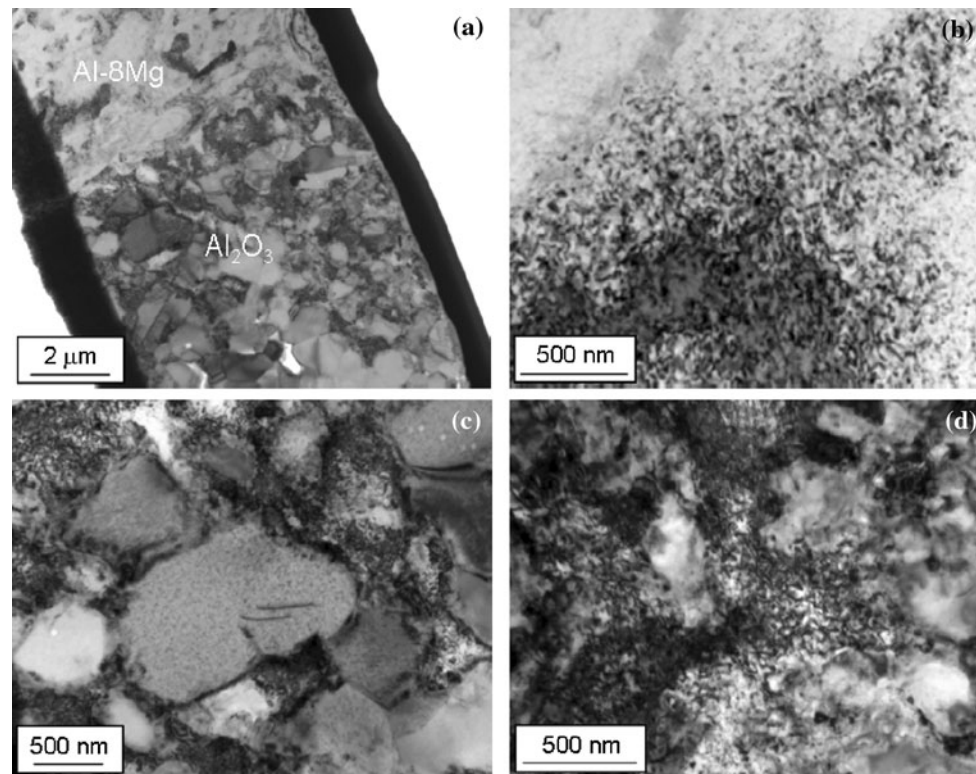
Fig. 9 TEM micrographs of the IPCs at the metal–ceramic interface after ballistic testing: **a** the metal–ceramic interface; **b** the Al–Mg alloy; **c** the ceramic struts from a DoP sample and **d** the ceramic struts from an SHPB sample

longitudinal stress waves [25]. Compared with the damage observed in the IPCs ballistically tested without a ceramic front face [20], very little plastic deformation and cracking was observed in the IPC layer in the metal-bonded ceramic-IPC components. One surface crack that propagated preferentially in the ceramic struts was seen on the fractured surface, Fig. 8c and d, this was bridged by at least one spherical metal relic (presumably from a ruptured cell in the ceramic foam). As observed previously [20], the interpenetrating metal structure contributed to the damage tolerance of the IPCs by bridging the cracks formed. Some very fine, partially developed radial cracks were observed from the top surface of the dense Al_2O_3 front face, Fig. 8e; from Fig. 8f, a higher magnification view, it can be seen that the Al_2O_3 fractured primarily in an intergranular manner. It would appear that the ceramic front face absorbed most of the kinetic energy from the round whilst the IPCs reduced the acoustic impedance mismatch with the Al backing.

An image of a TEM sample specifically prepared using the dual beam FIB from the metal–ceramic interface is shown in Fig. 9a; the interface remained intact without any porosity or interfacial debonding. The observation showed that tremendous numbers of dislocations were formed in the metal alloy with both SHPB and DoP testing as expected; an example is shown in Fig. 9b. A large number of dislocations were also formed in the metallic phase along the Al_2O_3 grain boundaries, Fig. 9c, which could have assisted dramatically the plastic deformation within the ceramic struts under the impact; the presence of the thin layer metallic phase along the Al_2O_3 grain boundaries is a direct result of the excellent wetting between the molten Al–Mg alloy and the Al_2O_3 grains and the molten metal infiltration. However, few dislocations was observed in the Al_2O_3 grains in the ceramic struts in the DoP sample, Fig. 9c and none were observed in the struts in the SHPB-tested samples, Fig. 9d. This might result in localised fracture in the ceramic struts. It appears that the plastic deformation in the IPC samples may be attributed to the presence of dislocations in the metallic phase both in the alloy and the Al_2O_3 grain boundaries, and localised fracture in the ceramic struts.

Conclusion

Ceramic-faced, metal–ceramic IPCs have been produced in situ using a pressureless infiltration technique and two different approaches, viz., a metal-bonded and a ceramic-bonded configuration. The former worked very well indeed; the latter needs further development if it is to be pursued. The ballistic performance of the metal-bonded components was evaluated using both a laboratory high

strain rate approach, SHPB, and DoP measurements, the latter undertaken using steel tipped, 7.62 mm, AP rounds. The results have shown that the metal-bonded ceramic-IPC configuration prevented the rounds from penetrating through to the aluminium backing for the DoP measurements, i.e. the DoP values were zero. Whilst most of the samples fractured and often detached from the backing plate, the bond between the ceramic front face and IPC always remained intact. One sample survived with only spall damage to the dense Al_2O_3 front face. It is surmised that the IPC layer provides a reduction in the impedance mismatch from the ceramic front to the Al backing. The plastic deformation in the IPCs was observed to result from the presence of dislocations allowing the metal phase to deform whilst the ceramic phase coped with the distortion via localised cracking. The presence of metal bridges across the crack fronts helped to increase the damage tolerance in the IPCs.

References

1. Tjong SC, Ma ZY (2000) Mater Sci Eng R 29:49
2. Lear MH, Sankar BV (1999) J Mater Sci 34:4181. doi: 10.1023/A:1004630230780
3. Tasdemirci A, Hall IW (2007) Int J Imp Eng 34:1797
4. Gooch WAC, Burkins BHC, Palicka MS, Rubin R, Ravichandran JR (1999) Mater Sci Forum 308–311:614
5. Bhagat RB, Amateau MF, House MB, Meinert KC, Nisson P (1992) J Compos Mater 26:1578
6. Manoharan M, Lewandowski JJ (1990) Acta Metall Mater 38:489
7. Rawal SP (2001) JOM 53:14
8. Lee WS, Sue WC (2000) J Compos Mater 34:1821
9. Doong JL, Lin SNS, Marcus HL (1992) J Mater Sci 27:1369. doi: 10.1007/BF01142056
10. Niu LB, Hojamberdiev M, Xu YH, Wu H (2010) J Mater Sci 45:4532. doi:10.1007/s10853-010-4549-6
11. Lo SHJ, Dionne S, Sahoo M, Hawthorne HM (1992) J Mater Sci 27:5681. doi:10.1007/BF01119723
12. Clarke DR (1992) J Am Ceram Soc 75:739
13. Mortensen A (2000) Comprehensive composite materials. In: Clyne TW (ed) Metal matrix composites. Elsevier, Amsterdam, p 521
14. Chang H, Higginson RL, Binner JGP. J Mater Sci. doi:10.1007/s10853-009-3983-9
15. Calderon NR, Voytovych R, Narciso J, Eustathopoulos N (2010) J Mater Sci 45:4345. doi:10.1007/s10853-010-4358-y
16. Chang H, Higginson RL, Binner JGP (2009) J Microsc 233:132
17. Soundararajan R, Kuhn G, Atisivan R, Bose S, Bandyopadhyay A (2001) J Am Ceram Soc 84:509
18. Liu JW, Zheng ZX, Wang JM, Wu YC, Tang WM, Lü J (2008) J Alloy Compd 465:239
19. Wang SR, Wang YZ, Wang Y, Geng HR, Chi CQ (2007) J Mater Sci 42:7812. doi:10.1007/s10853-007-1591-0
20. Chang H, Binner JGP, Higginson RL (2011) Mater Sci Eng A. doi:10.1016/j.msea.2010.12.016
21. Binner JGP, Chang H, Higginson RL (2009) J Eur Ceram Soc 29:837
22. Sepulveda P, Binner JGP (1999) J Eur Ceram Soc 19:2059
23. Kolsky H (1949) Proc Phys Soc Lond Ser B 62:676
24. Madhu V, Ramanjaneyulu K, Balakrishna Bhat T, Gupta NK (2005) J Impact Eng 32:337
25. Sherman D, Ben-Shushan T (1998) Int J Imp Eng 21:245
26. López-Puente J, Arias A, Zaera R, Navarro C (2005) Int J Imp Eng 32:321
27. Straßburger E, Lexow B, Beffort O, Jeanquartier R (2001) 19th international symposium of ballistics, Interlaken, Switzerland
28. Lee M, Yoo YH (2001) Int J Imp Eng 25:819
29. Forquin P, Tran L, Louvigné PF, Rota L, Hild F (2003) Int J Imp Eng 28:1061